Surface Science 657 (2017) 63–68

Contents lists available at ScienceDirect

Surface Science

journal homepage: www.elsevier.com/locate/susc

One-atom-layer 4×4 compound in (Tl, Pb)/Si(111) system

A.N. Mihalyuk[a,b], C.R. Hsing[c], C.M. Wei[c], D.V. Gruznev[a], L.V. Bondarenko[a], A.Y. Tupchaya[a], A.V. Zotov[a,b,d], A.A. Saranin[a,b,*]

[a] Institute of Automation and Control Processes FEB RAS, 5 Radio Street, 690041 Vladivostok, Russia
[b] School of Natural Sciences, Far Eastern Federal University, 690950 Vladivostok, Russia
[c] Institute of Atomic and Molecular Sciences, Academia Sinica, P.O. Box 23-166, Taipei, Taiwan
[d] Department of Electronics, Vladivostok State University of Economics and Service, 690600 Vladivostok, Russia

ARTICLE INFO

Keywords:
Silicon
Thallium
Lead
2D compounds
Scanning tunneling microscopy
DFT calculations

ABSTRACT

An ordered 4×4-periodicity 2D compound has been found in the (Tl, Pb)/Si(111) system and its composition, structure and electronic properties have been characterized using low-energy electron diffraction, scanning tunneling microscopy observations and density-functional-theory calculations. The compound has been concluded to contain 9 Tl atoms and 12 Pb atoms per 4×4 unit cell, i.e., 0.56 ML of Tl and 0.75 ML of Pb. Structural model was proposed for the 4×4-(Tl, Pb) compound where building blocks are a hexagonal array of 12 Pb atoms, a triangular array of 6 Tl atoms and a Tl trimer. The proposed structure has a C_3 symmetry and occurs in the two equivalent orientations. The electron band structure of the compound contains two metallic spin-split surface-state bands. Bearing in mind the advanced properties of the known $\sqrt{3} \times \sqrt{3}$ 2D compound in the same (Tl, Pb)/Si(111) system (i.e., combination of giant Rashba effect and superconductivity), the found 4×4-(Tl, Pb) compound is believed to be a promising object for exploration of its superconductive properties.

1. Introduction

Discovery of graphene has stimulated the current interest to atomically thin, two-dimensional (2D) materials which might exhibit unique properties not observed in the bulk materials. Metal-induced surface reconstructions on silicon and germanium (i.e., metal films of a monolayer or submonolayer on silicon or germanium) are vivid examples. Most of the studies in this field have been restricted to the reconstructions built of a single atomic species. Natural expansion of the research area is the exploration of the 2D multi-component systems. Efficiency of this approach has been proved in the very recent studies of the multi-component 2D layers on silicon [1–12] and germanium [13,14]. In particular, adding appropriate adsorbates (e.g., In, Tl, Na, or Cs) to originally structurally and electronically poor Au/Si(111) $\sqrt{3} \times \sqrt{3}$ reconstruction converts it into a perfect 2D electron-gas system [3] with spin-split metallic surface-state bands [4,5]. A still greater promise is associated with the ordered 2D compounds or alloys which can be considered as a novel class of 2D materials [1]. For example, the (Sn, Ag)/Si(111)2×2 [1] and (Tl, Sn)/Si(111)$\sqrt{3} \times \sqrt{3}$ [11] systems show up to be metallic with steep dispersion of the surface-state bands where when crossing the Fermi level yields an electron velocity ~8×10^5 m/s that is comparable to the value of ~1×10^6 m/s reported for graphene. In addition, electronic properties of the (Sn, Ag)/Si(111)2×2 can be tuned from metallic to semiconducting by adsorption of additional Ag onto the surface [1]. A number of 2D compounds (e.g., (Bi, Na)/Si(111)$\sqrt{3} \times \sqrt{3}$ [8,15], (Tl, Pb)/Si(111)$\sqrt{3} \times \sqrt{3}$ [8], (Au, Al)/Si(111)2×2 [10]) demonstrate a giant Rashba effect with spin splitting of the metallic bands near the Fermi level ΔE_F ~150–250 meV. Among them, the (Au, Al)/Si(111)2×2 exhibits an unusual anisotropic spin texture [10]. The (Tl, Pb)/Si(111)$\sqrt{3} \times \sqrt{3}$ compound has been found to combine a giant Rashba effect and two-dimensional superconducting transport properties [8], so offers the potential to the superconducting spintronics [16].

Bearing in mind these advanced properties of the (Tl, Pb)/Si(111) system, we have examined it in a more detail. In addition to the known (Tl, Pb)/Si(111) $\sqrt{3} \times \sqrt{3}$, one more ordered compound having 4×4 periodicity has been found. It plausibly contains 9 Tl atoms and 12 Pb atoms per 4×4 unit cell, i.e., 0.56 ML of Tl and 0.75 ML of Pb, the total metal coverage being 1.31 ML. The structural model has been derived which incorporates a hexagonal array of 12 Pb atoms, triangular array of 6 Tl atoms and a Tl trimer as the structure building blocks. The 2D compound has a C_3 symmetry, hence occurs in the two possible orientations. Surmounting a barrier of 77 meV, it can twist from one orientation to another through an intermediate structure having a C_{3v} symmetry. The (Tl, Pb)/Si(111)4×4 compound has been found to be metallic with two spin-split metallic surface-state bands. The com-

* Corresponding author at: Institute of Automation and Control Processes FEB RAS, 5 Radio Street, 690041 Vladivostok, Russia.
E-mail address: saranin@iacp.dvo.ru (A.A. Saranin).

http://dx.doi.org/10.1016/j.susc.2016.11.004
Received 3 October 2016; Received in revised form 1 November 2016; Accepted 3 November 2016
Available online 27 November 2016
0039-6028/

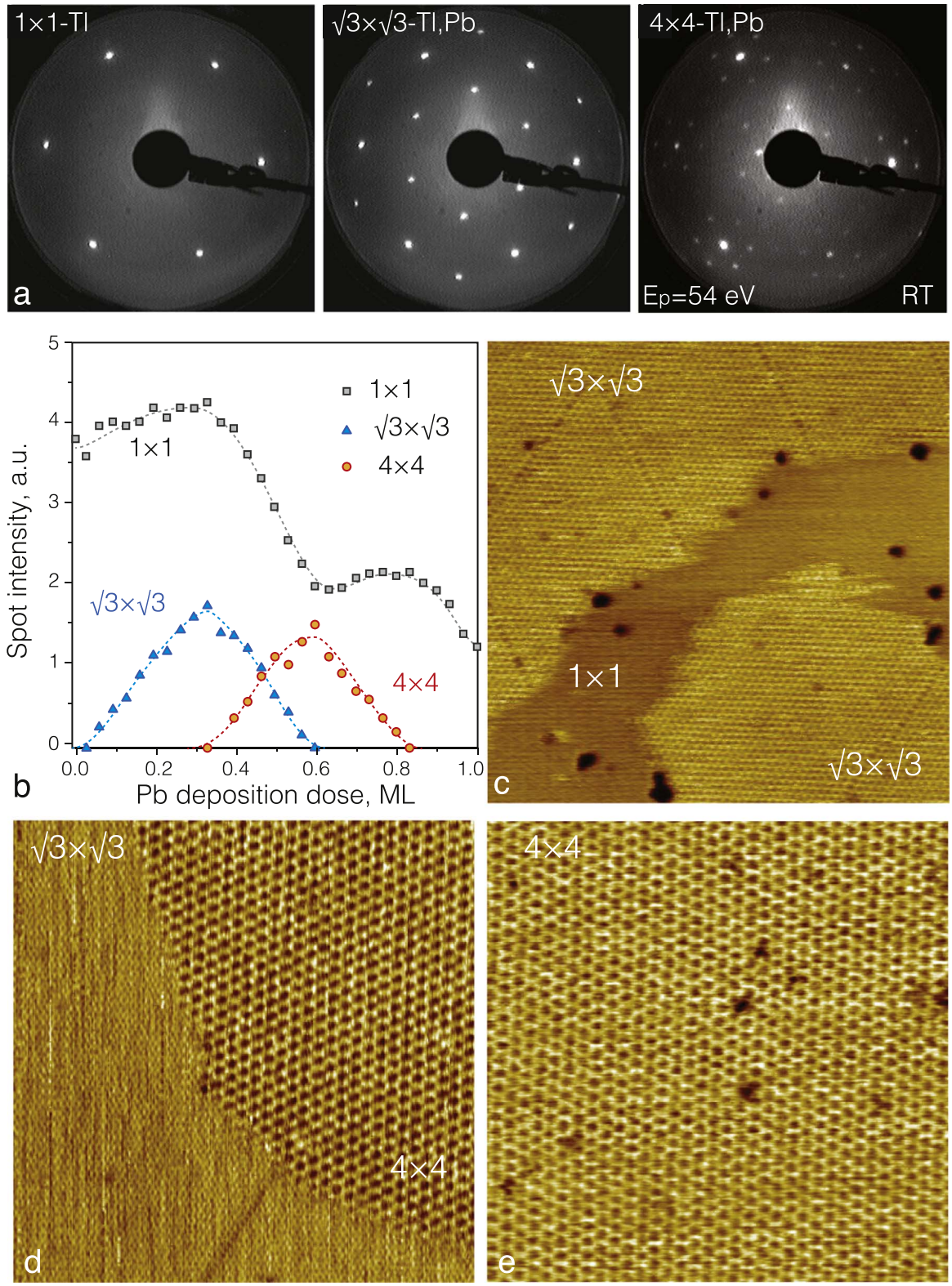

Fig. 1. (a) LEED patterns (E_p = 54 eV) from pristine Tl/Si(111)1×1 surface and 2D (Tl, Pb)/Si(111)$\sqrt{3} \times \sqrt{3}$ and (TL, Pb)/Si(111)4×4 compounds acquired at RT. (b) Evolution of the LEED spot intensities in the course of structural transformations induced by Pb deposition onto Tl/Si(111)1×1 surface held at RT. (c) and (d) 50×50 nm^2 STM images (acquired at −0.8 V, 0.6 nA and +0.5 V, 1 nA, respectively) showing the mixed $1 \times 1/\sqrt{3} \times \sqrt{3}$ and $\sqrt{3} \times \sqrt{3}$/4×4 surfaces, respectively. (e) 50×50 nm^2 STM image (acquired at +1.0 V, 1.0 nA) of the (Tl, Pb)/Si(111)4×4 surface.

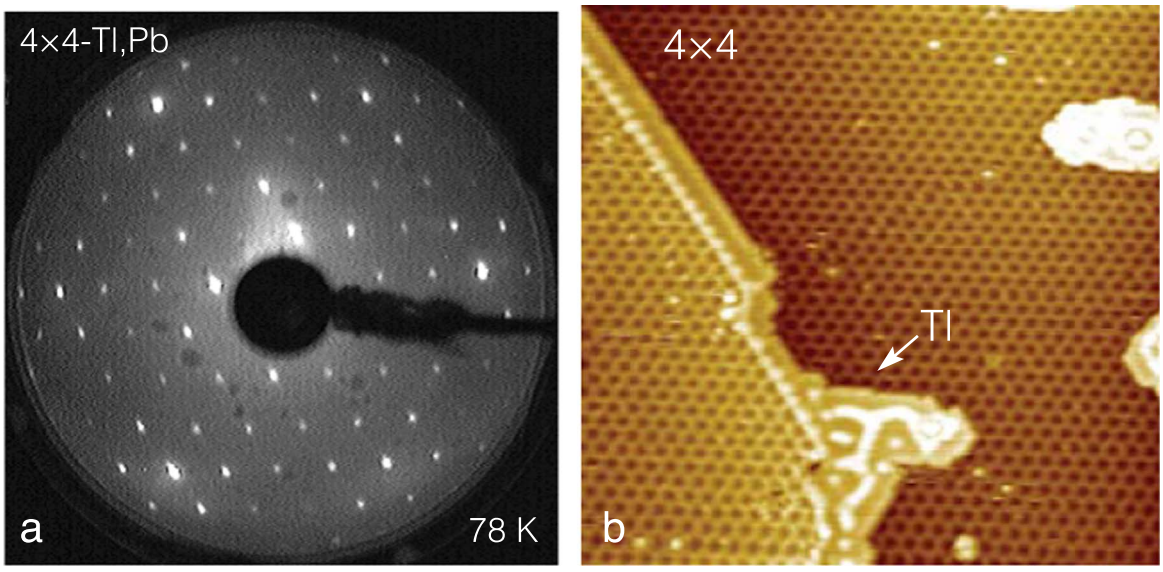

Fig. 2. (a) LEED pattern (E_p = 54 eV) and (b) 50×50 nm^2 STM image (+1.4 V, 0.4 nA) of the (Tl,Pb)/Si(111)4×4 surface acquired at 78 K. The Tl double layer along the step edge is indicated by the arrow.

pound is believed to be a promising object for low-temperature transport measurements for exploration of the superconducting properties of the (Tl, Pb)/Si(111) system.

2. Experimental and calculation details

Our experiments were performed with Omicron MULTIPROBE system operated in an ultrahigh vacuum (~2.5×10^{-10} mbar). Atomically-clean Si(111)7×7 surface was prepared *in situ* by flashing to 1280 °C after the sample was first outgassed at 600 °C for several hours. Tl and Pb were deposited from Ta tubes. The amounts of deposited Tl and Pb were evaluated from the deposition times using calibration based on the formation of the known reconstructions, namely Si(111)1×1-Tl phase containing 1.0 ML of Tl and Si(111)$\sqrt{3}\times\sqrt{3}$-(Tl, Pb) compound incorporating 0.33 ML of Pb and 1.0 ML of Tl. Typical accuracy of such evaluations is on the order of ~20%. Structure of the forming (Tl, Pb)/Si(111) surfaces was monitored using low-energy electron diffraction (LEED) and scanning tunneling microscopy (STM) observations. STM images were acquired in a constant-current mode with a mechanically cut PtIr tip after annealing in vacuum.

Our calculations were based on DFT as implemented in the Vienna *ab initio* simulation package VASP [17,18] using a planewave basis set. The projector-augmented wave approach [19] was used to describe the electron-ion interaction and the generalized gradient approximation (GGA) of Perdew, Burke, and Ernzerhof (PBE) [20] was employed as the exchange-correlation functional. The scalar relativistic effect and the spin-orbit interaction (SOI) were taken into account. To simulate the Tl-Pb reconstructions on Si(111) we used a slab consisting of four bilayers (BL) of silicon, at the PBE-optimized bulk Si lattice constant. Hydrogen atoms were used to passivate the Si dangling bonds at the bottom of the slab. The atomic positions of adsorbed atoms and atoms of Si layers within the three BLs of the slab were optimized. Silicon atoms of the deeper layers were kept fixed at the bulk crystalline positions. The kinetic cutoff energy was 400 eV, and a 5×5×1 *k*-point mesh was used to sample the surface Brillouin zone. The geometry optimization is performed until the residual force on atoms was smaller than 10 meV/Å.

3. Results and discussion

Formation of the Tl-Pb compounds on the Si(111) surface is illustrated in Fig. 1 which summarizes the results of LEED and STM observations. The process was started with preparation of the high-quality Tl/Si(111)1×1 template surface which was obtained by adsorbing 1.0 monolayer (ML) of Tl onto the Si(111)7×7 surface held at about 300 °C [1 ML=7.8×10^{14} cm^{-2}]. The 1×1-Tl phase is known to contain a layer of Tl atoms occupying every T_4 site on the bulk-truncated Si(111) substrate surface [21–23]. When Pb is deposited onto the Tl/Si(111) 1×1 surface held at room temperature (RT), regions of the Tl-Pb 2D compound having a $\sqrt{3}\times\sqrt{3}$ periodicity develop (Fig. 1c). The regions merge together and cover the entire surface after deposition of ~1/3 ML of Pb (Fig. 1b), in agreement with the previous reports [8,9]. The (Tl,Pb)/Si(111)$\sqrt{3}\times\sqrt{3}$ surface shows up in STM images as an array with a honeycomb-like inner arrangement (Fig. 1c). As determined in Ref. [8], the Tl-Pb compound layer is composed of honeycomb-chained trimers of Tl atoms with Pb atoms occupying the T_4 sites in the center of each honeycomb unit. If Pb deposition is continued, the next Tl-Pb 2D compound displaying a 4×4 periodicity starts to form (Figs. 1b and d). The 4×4 LEED pattern demonstrates the highest intensity after deposition of slightly more than 0.6 ML of Pb (Fig. 1b). In the STM images, the (Tl, Pb)/Si(111)4×4 surface also exhibits a honeycomb-like appearance (Fig. 1e). In the 4×4 LEED pattern, the 1/4th extra reflections are bright only in the vicinity of the main reflections (Fig. 1a). However, upon cooling the sample to 78 K, the sharp 4×4 LEED pattern is observed where all the 1/4th reflections are clearly seen (Fig. 2 a). Meanwhile, the STM appearance of the surface does not change noticeably (Fig. 2b). The only new feature is the appearance of the arrays occupied by a double Tl layer [24–26] which develop preferentially along the step edges. Occurrence of the excess Tl implies that formation of the (Tl, Pb)-4×4 compound involves substitution of certain portion of Tl for Pb.

Following the hints that (i) Pb substitutes Tl, (ii) Pb coverage is above 0.6 ML and (iii) STM demonstrates C_{3v} symmetry of the surface, we have checked a wide set of the (Tl, Pb)/Si(111)4×4 models of various Tl-Pb compositions using DFT calculations. The calculations prove that the structure formation energy decreases with substitution of Tl for Pb and the most optimal pathway is that when the total metal coverage remains essentially unchanged. This means that the number of the substituted Tl atoms is approximately the same as the number of

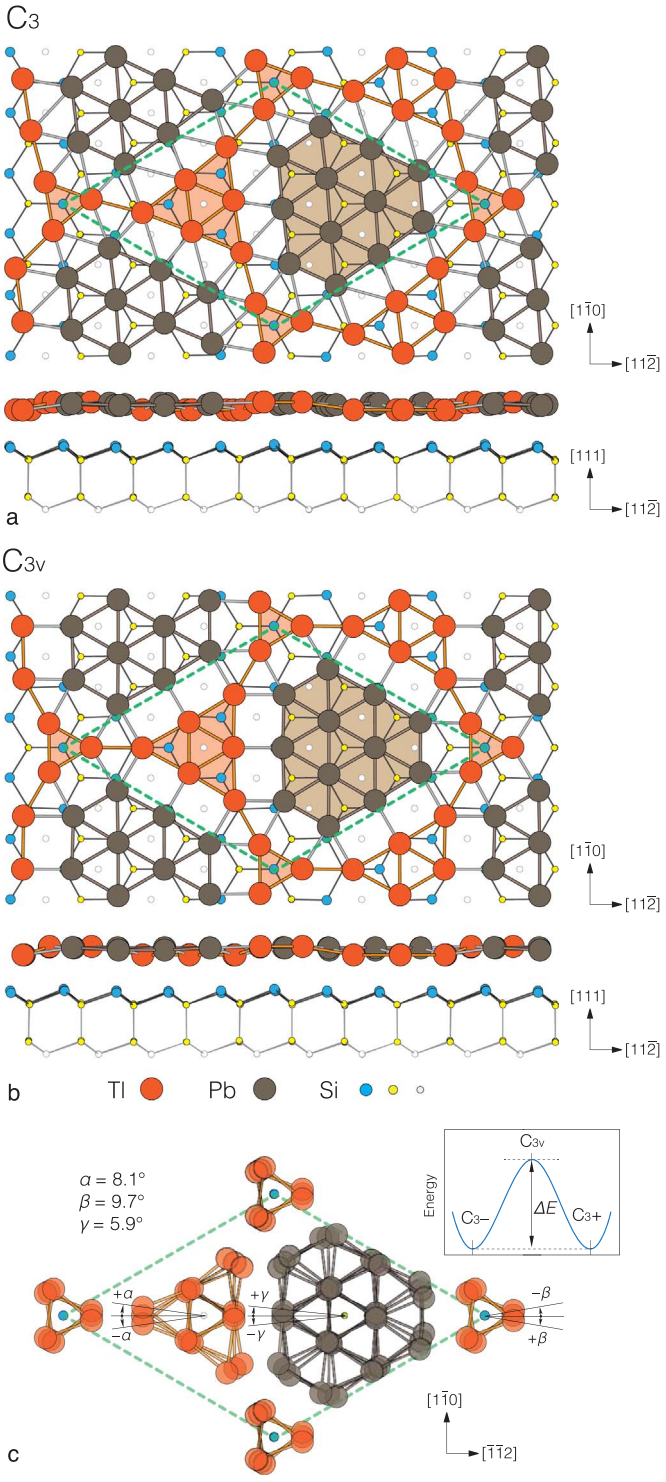

Fig. 3. Structure models of the Tl, Pb)/Si(111)4×4 having (a) C_3 and (b) C_{3v} symmetry. (c) Schematic diagram illustrating the transition between C_3 structures in the two possible orientation with a C_{3v} structure as an intermediate stage.

the adopted Pb atoms. Thus, it has been appeared that the most plausible Tl-Pb compounds contain 9 Tl atoms and 12 Pb atoms per 4×4 unit cell, i.e., 0.56 ML of Tl and 0.75 ML of Pb, the total metal coverage being 1.31 ML. Remind that the preceding $\sqrt{3} \times \sqrt{3}$-(Tl, Pb) phase contained 1.0 ML of Tl and 0.33 ML of Pb, hence the total metal coverage was 1.33 ML. One can note that the model Pb coverage of 0.75 ML exceeds the value of ~0.6 ML where the 4×4 LEED intensity curve displays the maximum (see Fig. 1b). This can be attributed to the presence of the Tl double-layer patches like that shown in Fig. 2b. As a result, the 4×4-(Tl, Pb) compound never occupies the whole surface area and its Pb contents is greater than the averaged density of Pb atoms at the surface.

Among the C_{3v} structure models with the optimal composition, the one shown in Fig. 3b has the lowest formation energy. However, if the system is allowed to relax in the absence of mirror-symmetry limitations it evolves to the one having C_3 symmetry as shown in Fig. 3a. Formation energy of the C_3 model is lower that that of the C_{3v} model by ~77 meV per 4×4 unit cell when PBE approximation is used. For LDA approximation this value is somewhat lower and is ~50 meV. Both models have a very similar atomic arrangement being composed of the same building blocks. In the models, 12 Pb atoms form a hexagonal array in which Pb atoms occupy positions close to the on-top (T_1) sites. The Pb-atom array has a shape of the hexagon which can be visualized also as a truncated triangle. Nine Tl atoms are arranged into the two structural elements. The first element contains 6 Tl atoms forming an array of triangular shape where Tl atoms occupy positions close to the T_4 sites. The other 3 Tl atoms form a trimer centered in the T_1 site while Tl atoms are located close to the H_3 sites. Table 1 shows structural parameters of the two models. Lacking of the mirror symmetry in the C_3-model is due to the twist of structural elements, namely, the Pb-atom array is twisted by 5.9°, the Tl six-atom triangle by 8.1° and the Tl trimer by 9.7° with respect to the orientations of their counterparts in the C_{3v}-model. Fig. 3c illustrates occurrence of the C_3-model structure in the two equivalent orientations with twisting of structural elements either clockwise or counter-clockwise. One can also see in Fig. 3c that transition of the C_3-structure from one orientation to another occurs through the C_{3v}-structure as an intermediate stage. The transition implies surmounting a barrier. Remind that the maximal barrier value obtained within PBE approximation is ~77 meV. Nevertheless, this is a relatively small value and one could expect that the structure is in a continuous twisting between two orientations even at relatively low temperatures.

As a test for the validity of the proposed models, we have compared simulated STM images obtained for the models with the experimental high-resolution STM images where the fine structural features can be seen. The results of the comparison are summarized in Fig. 4. One can see that the simulated STM images for the C_3- and C_{3v}-models (Figs. 4 b and c) are almost identical as a natural sequence of their structural similarity. In turn, both models demonstrate a close resemblance with the experimental STM images (Fig. 4a) that sounds supportive for the correct choice of the models.

Having plausible structure models, we have calculated their electron band structures shown in Fig. 5. Fig. 5a shows the calculated band structure for the C_3-model and Fig. 5b shows that for the C_{3v}-model. The band structures are represented by the dispersion curves along the $\overline{\Gamma}$-$\overline{M}$-$\overline{\Gamma}$ and $\overline{\Gamma}$-$\overline{K}$-$\overline{M}$-$\overline{K}$ directions of the 4×4 surface Brillouin zone

Table 1
Structural parameters of the C_3 and C_{3v} models shown in Fig. 3.

Model	Tl Triangle			Tl Trimer			Pb Hexagon		
	d_{Tl-Tl}, Å	Δh_{Tl-Si}, Å	α, °	d_{Tl-Tl}, Å	Δh_{Tl-Si}, Å	β, °	d_{Pb-Pb}, Å	Δh_{Pb-Si}, Å	γ, °
C_3	3.26–3.39	2.39	8.1	3.10	2.86	9.7	3.23–3.48	2.75	5.9
C_{3v}	3.22–3.45	2.36	0	3.06	2.88	0	3.18–3.35	2.81	0

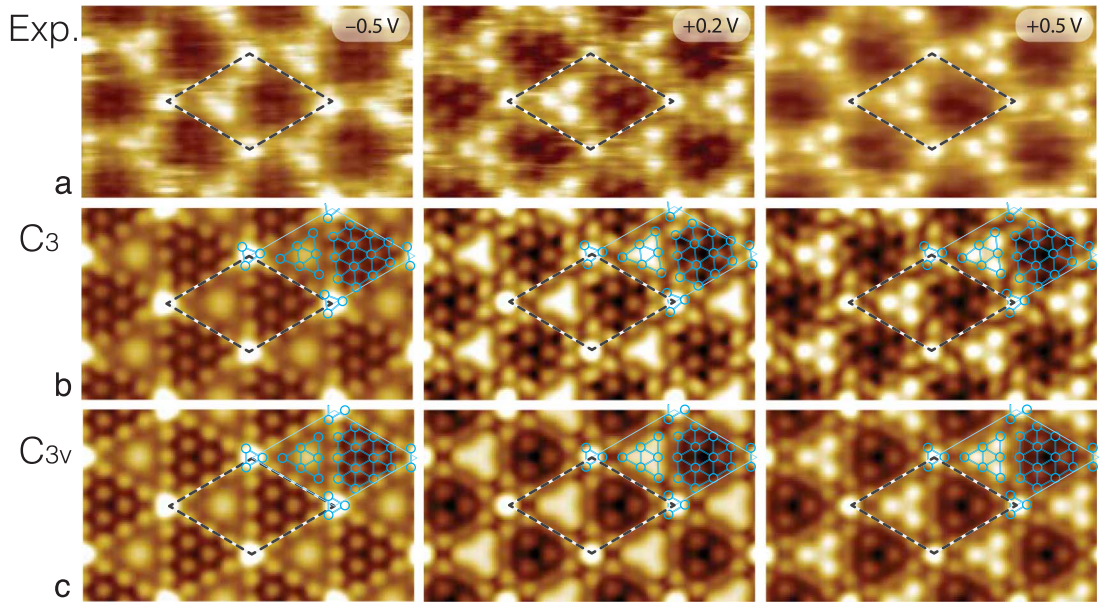

Fig. 4. Comparison of (a) experimental STM images acquired at −0.5 V, +0.2 V and +0.5 V biases with the corresponding simulated STM images for (b) C_3- and (c) C_{3v}-models of the (Tl, Pb)/Si(111)4×4 surface. The 4×4 unit cells are outlined. The main structural elements of the models (Pb-atom array, Tl-atom triangular array and Tl trimers) are superposed onto the simulated STM images to illustrate the origin of the STM features.

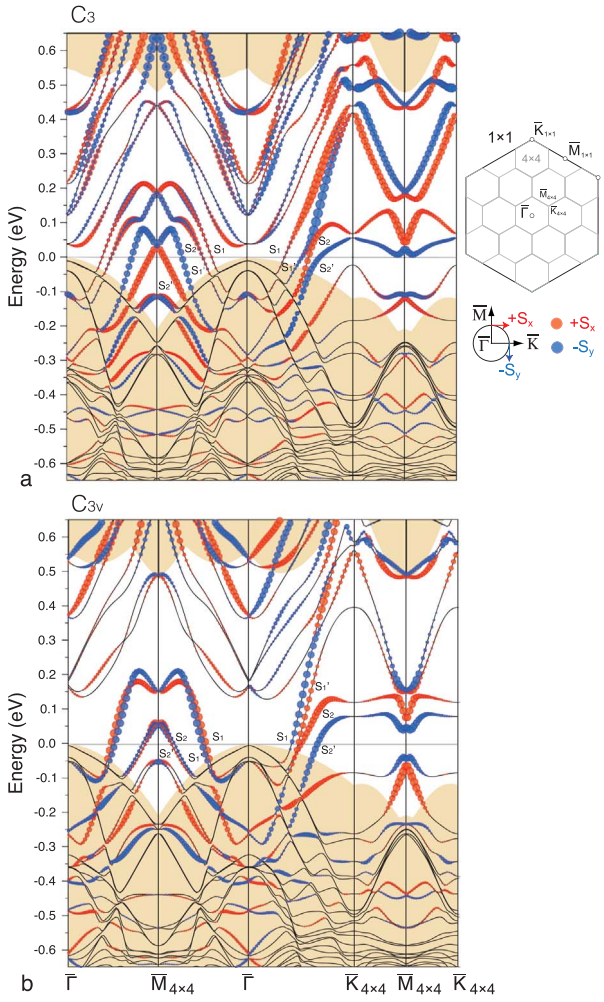

Fig. 5. Electron band structures calculated for (a) C_3- and (b) C_{3v}-models of the (Tl, Pb)/Si(111)4×4 phase.

(SBZ) as indicated in the schematics in Fig. 5. One can see that both structures contains two spin-split metallic surface-state bands, denoted *S*1 (*S*1′) and *S*2 (*S*2′). Remarkably, spin splitting in the case of the C_3-model structure is noticeably greater than that for the C_{3v} structure (see Table 2). It is worth noting also that despite the difference in the periodicity the calculated band structure of the 4×4-(Tl, Pb) compounds is qualitatively akin those calculated and experimentally determined with ARPES for the $\sqrt{3} \times \sqrt{3}$-(Tl, Pb) compound [8].

4. Conclusions

In conclusion, we have extended the list of the 2D compounds in the (Tl, Pb)/Si(111) system by finding the Tl-Pb compounds having a 4×4 periodicity. Composition, atomic structure and electronic properties of the 4×4-(Tl, Pb) compound has been characterized using combination of LEED and STM observations and DFT claculations. The compound has been concluded to contain 9 Tl atoms and 12 Pb atoms per 4×4 unit cell, i.e., 0.56 ML of Tl and 0.75 ML of Pb, the total metal coverage being 1.31 ML. Its atomic model has been proposed which is built of three basic blocks, including a hexagonal array of 12 Tb atoms, triangular array of 6 Pb atoms and a Pb trimer. The 4×4-(Tl, Pb) compound occurs in the two equivalent orientations and is plausibly twisting between them even at relatively low temperatures, taking into account a low barrier of ~77 meV. Compound has been found to be metallic with two spin-split metallic surface-state bands.

We believe that the (Tl, Pb)/Si(111) compound is a promising object for low-temperature transport measurements for exploration of the superconducting properties of the (Tl, Pb)/Si(111) system. In particular, it allows to address the effect of the Tl-Pb composition and structure on the properties of the 2D-compound superconductor. Compared to the $\sqrt{3} \times \sqrt{3}$-(Tl, Pb), the 4×4-(Tl, Pb) compound is more Pb-rich. However, it is difficult to suggest in advance, if this would enhance superconducting properties or not. Remind that the critical temperature for the $\sqrt{3} \times \sqrt{3}$-(Tl, Pb) compound is 2.3 K [9], for the Pb films thicker than 8 ML it approaches a bulk value of ~7 K [27], for the one-atom-layer Pb film on Si(111) the transport measurements yield 1.1 K [28], while the STS-based measurements yield 1.52 K and 1.83 K, depending on the structure and density of Pb-atom layer [29].

Table 2
Calculated values of the spin split parameters of S_1 and S_2 zones in the $\overline{\Gamma} - \overline{M}$ and $\overline{\Gamma} - \overline{K}$ directios in the vicinity of Fermi level.

Model	$\overline{\Gamma} - \overline{M}$				$\overline{\Gamma} - \overline{K}$			
	S_1		S_2		S_1		S_2	
	Δk, Å^{-1}	ΔE, meV	Δk, Å^{-1}	ΔE, meV	Δk, Å^{-1}	ΔE, meV	Δk, Å^{-1}	ΔE, meV
C_3	0.023	55	0.047	105	0.045	77	0.027	52
C_{3v}	0.009	34	0.008	17	0.017	48	0.042	128

Acknowledgements

The experimental part of the work was supported by the Russian Science Foundation under Grant 14-12-00479. Band structure calculations were partly supported by the Ministry of Science and Education, Russian Federation, under Grant NSh-6889.2016.2 and the Ministry of Science and Technology, Taiwan, under Grant NSC 103-2923-M-001-005-MY3.

References

[1] J.R. Osiecki, H.M. Sohail, P.E.J. Eriksson, R.I.G. Uhrberg, Experimental and theoretical evidence of a highly ordered two-dimensional Sn/Ag alloy on Si(111), Phys. Rev. Lett. 109 (2012) 057601.
[2] D.V. Gruznev, I.N. Filippov, D.A. Olyanich, D.N. Chubenko, I.A. Kuyanov, A.A. Saranin, A.V. Zotov, V.G. Lifshits, Si(111)-α-$\sqrt{3} \times \sqrt{3}$-Au phase modified by In adsorption: stabilization of a homogeneous surface by stress relief, Phys. Rev. B 73 (2006) 115335.
[3] J.K. Kim, K.S. Kim, J.L. McChesney, E. Rotenberg, H.N. Hwang, C.C. Hwang, H.W. Yeom, Two-dimensional electron gas formed on the indium-adsorbed Si(111)$\sqrt{3} \times \sqrt{3}$-Au surface, Phys. Rev. B 80 (2009) 075312.
[4] L.V. Bondarenko, D.V. Gruznev, A.A. Yakovlev, A.Y. Tupchaya, D. Usachov, O. Vilkov, A. Fedorov, D.V. Vyalikh, S.V. Eremeev, E.V. Chulkov, A.V. Zotov, A.A. Saranin Large spin splitting of metallic surface-state bands at adsorbate-modified gold/silicon surfaces, Sci. Rep. 3 (2013) 1826.
[5] L.V. Bondarenko, A.V. Matetskiy, A.A. Yakovlev, A.Y. Tupchaya, D.V. Gruznev, M.V. Ryzhkova, D.A. Tsukanov, E.A. Borisenko, E.N. Chukurov, N.V. Denisov, O. Vilkov, D.V. Vyalikh, A.V. Zotov, A.A. Saranin, Effect of Na adsorption on the structural and electronic properties of Si(111)$\sqrt{3} \times \sqrt{3}$-Au surface, J. Phys. C ond. Matt. 26 (2014) 055009.
[6] N.V. Denisov, E.N. Chukurov, Y.V. Luniakov, O.A. Utas, S.G. Azatyan, A.A. Yakovlev, A.V. Zotov, A.A. Saranin, Two-dimensional bismuth-silver structures on Si(111), Surf. Sci. 623 (2014) 17.
[7] N.V. Denisov, A.A. Alekseev, O.A. Utas, S.G. Azatyan, A.V. Zotov, A.A. Saranin, Bismuth-indium two-dimensional compounds on Si(111) surface, Surf. Sci. 651 (2016) 105.
[8] D.V. Gruznev, L.V. Bondarenko, A.V. Matetskiy, A.A. Yakovlev, A.Y. Tupchaya, S.V. Eremeev, E.V. Chulkov, J.P. Chou, C.M. Wei, M.Y. Lai, Y.L. Wang,, A.V. Zotov, A.A. Saranin, A strategy to create spin-split metallic bands on silicon using a dense alloy layer, Sci. Rep. 4 (2014) 4742.
[9] A.V. Matetskiy, S. Ichinokura, L.V. Bondarenko, A.Y. Tupchaya, D.V. Gruznev, A.V. Zotov, A.A. Saranin, R. Hobara, A. Takayama, S. Hasegawa, Two-dimensional superconductor with a giant Rashba effect:one-atom-layer Tl-Pb compound on Si(111), Phys. Rev. Lett. 115 (2015) 147003.
[10] D.V. Gruznev, L.V. Bondarenko, A.V. Matetskiy, A.Y. Tupchaya, E.N. Chukurov, C.R. Hsing, C.M. Wei, S.V. Eremeev, A.V. Zotov, A.A. Saranin, Atomic structure and electronic properties of the two-dimensional (Au,Al)/Si(111)2×2 compound, Phys. Rev. B 92 (2015) 245507.
[11] D.V. Gruznev, L.V. Bondarenko, A.V. Matetskiy, A.Y. Tupchaya, A.A. Alekseev, C.R. Hsing, C.M. Wei, S.V. Eremeev, A.V. Zotov, A.A. Saranin, Electronic band structure of a Tl/Sn atomic sandwich on Si(111), Phys. Rev. B 91 (2015) 035421.
[12] D.V. Gruznev, L.V. Bondarenko, A.V. Matetskiy, A.N. Mihalyuk, A.Y. Tupchaya, O.A. Utas, S.V. Eremeev, C.R. Hsing, J.P. Chou, C.M. Wei, A.V. Zotov, A.A. Saranin, Synthesis of two-dimensional Tl_xBi_{1-x} compounds and Archimedean encoding of their atomic structure, Sci. Rep. 6 (2016) 19446.
[13] H. Sohail, R.I.G. Uhrberg, Electronic and atomic structures of a Sn induced $3\sqrt{3} \times 3\sqrt{3}$ superstructure on the Ag/Ge(111)$\sqrt{3} \times \sqrt{3}$ surface, Surf. Sci. 644 (2016) 29.
[14] H. Sohali, R.I.G. Uhrberg, Experimental studies of an In/Pb binary surface alloy on Ge(111), Surf. Sci. 649 (2016) 146.
[15] S.V. Eremeev, E.N. Chukurov, D.V. Gruznev, A.V. Zotov, A.A. Saranin, Atomic arrangement and electron band structure of Si(111)-β-$\sqrt{3} \times \sqrt{3}$-Bi reconstruction modified by alkali-metal adsorption: *ab initio* study, J. Phys.: Cond. Matt. 27 (2015) 305003.
[16] J. Linder, J.W.A. Robinson, Superconducting spintronics, Nat. Phys. 11 (2015) 307.
[17] G. Kresse, J. Hafner, *Ab initio* molecular dynamics for liquid metals, Phys. Rev. B 47 (1993) 558.
[18] G. Kresse, D. Joubert, From ultrasoft pseudopotentials to the projector augmented-wave method, Phys. Rev. B 59 (1999) 1758.
[19] P.E. Blöchl, Projector augmented-wave method, Phys. Rev. B 50 (1994) 17953.
[20] J.P. Perdew, K. Burke, M. Ernzerhof, Generalized gradient approximation made simple, Phys. Rev. Lett. 77 (1996) 3865.
[21] S.S. Lee, H.J. Song, N.D. Kim, J.W. Chung, K. Kong, D. Ahn, H. Yi, B.D. Yu, H. Tochihara, Structural and electronic properties of thallium overlayers on the Si(111)-7×7 surface, Phys. Rev. B 66 (2002) 233312.
[22] T. Noda, S. Mizuno, J. Chung, H. Tochihara, T_4 site adsorption of Tl atoms in a Si(111)-(1×1)-Tl structure, determined by low-energy electron diffraction analysis, Jpn. J. Appl. Phys. 42 (2003) L319.
[23] N.D. Kim, C.G. Hwang, J.W. Chung, T.C. Kim, H.J. Kim, D.Y. Noh, Structural properties of a thallium-induced Si(111)-1×1 surface, Phys. Rev. B 69 (2004) 195311.
[24] L. Vitali, F.P. Leisenberger, M.G. Ramsey, F.P. Netzer, Thallium overlayers on Si(111): structures of a “new” group III element, J. Vac. Sci. Technol. A 17 (1999) 1676.
[25] L. Vitali, M.G. Ramsey, F.P. Netzer, Unusial growth phenomena of group III and group V elements on Si(111) and Ge(111) surfaces, Appl. Surf. Sci. 175/176 (2001) 146.
[26] L. Vitali, M.G. Ramsey, F.P. Netzer, Rotational epitaxy of a ‘soft’ metal overlayer on Si(111), Surf. Sci. 452 (2000) L281.
[27] W. Zhao, Q. Wang, M. Liu, W. Zhang, Y. Wang, M. Chen, Y. Guo, K. He, X. Chen, Y. Wang, J. Wang, X. Xie, Q. Niu, L. Wang, X. Ma, J.K. Jain, M.H.W. Chanc, Q.K. Xue, Evidence for Berezinskii-Kosterlitz-Touless transition in atomically flat two-dimensional Pb superconducting films, Sol. State Commun. 165 (2013) 59.
[28] M. Yamada, T. Hirahara, S. Hasegawa, Magnetoresistance measurements of a superconducting surface state of In-induced and Pb-induced structures on Si(111), Phys. Rev. Lett. 110 (2013) 237001.
[29] T. Zhang, P. Cheng, W.J. Li, Y.J. Sun, G. Wang, X.G. Zhu, K. He, L. Wang, X. Ma, X. Chen, Y. Wang, Y. Liu, H.Q. Lin, J.F. Jia, Q.K. Xue, Superconductivity in one-atomic-layer metal films grown on Si(111), Nat. Phys. 6 (2010) 104.